Thermal Performances of an Improved Package for Cryocooled Josephson Standards

Paolo Durandetto, Eugenio Monticone, Danilo Serazio, and Andrea Sosso

Abstract— **Complex cryogenics still represents a strong limitation to the spread of Josephson voltage standards, and cryogen-free cooling is particularly suitable to simplify their operation. The main downsides of liquid-helium-free systems are related to the chip thermalization: Indeed, at low temperature, the heat transfer between the chip and the coldplate of a cryocooler in vacuum is strongly affected by the quality of the interfaces. In order to increase the thermal performances of cryocooled programmable Josephson standards, we devised and tested a special cryopackage: The chip is embedded into a sandwich structure with high-thermal-conductivity materials subject to a controlled mechanical pressure to reduce the thermal contact resistances. A thin sapphire lamina placed upon the chip allows the heat to be dissipated from the top, thus creating an additional path for the thermal flow. A special bridgelike system with a screw is used as a reproducible torque-to-force converter to exert known pressures to the sandwich. Furthermore, we analyzed the effect of thermal contraction to the actual pressure exerted on the chip, showing a nonnegligible increase when cooled down to cryogenic temperature that can be calculated and corrected for.**

Index Terms— **Cryocooler, heat transmission, He-free refrigeration, programmable Josephson arrays, thermal resistance.**

I. Introduction

SEVERAL decades after the discovery of the Josephson effect [1], voltage standards based on this quantum phenomenon still represent one of the most complex and successful achievements of superconducting electronics. Hysteretic superconductor-insulator-superconductor (SIS) technology has proved successful to fabricate arrays with tens of thousands Josephson junctions generating up to 10 V, which enabled primary dc voltage calibrations to attain relative uncertainties as low as 10^{-11} [2]. At present, quantum voltage standard research is focused on the application of Josephson arrays to ac and arbitrary signals: Programmable Josephson voltage standards (PJVS) represent, so far, the most widely adopted technology to rapidly control the output voltage [3]. They use bias currents to activate/deactivate different segments with series connected junctions whose number follows a binary law, as in digital-to-analog converters of semiconductor electronics.

Refrigeration of Josephson voltage standards is generally achieved with liquid helium: This limits the spread of these quantum devices outside National Metrology Institutes, due to the increasing cost of liquid helium, driven by shortages rumors, and to the specific skills required for handling the potentially hazardous cryogen. Moreover, the difficulty of fabricating large and uniform arrays with high-critical-temperature superconductors, such as YBCO and the more recent MgB_2 [4], still prevents the development of reliable Josephson standards working at higher temperatures.

Due to the simpler operation, cryocoolers capable of reaching temperatures below 4 K bear a particular interest for Josephson standards, although several problems arise. The most relevant is related to thermal issues: The reduced cooling power and the high-vacuum environment of cryocoolers have important consequences on the behavior of devices, the more if a significant power is dissipated during the experiment. When a Josephson array is operated, it warms up because of the received RF and dc bias currents, raising the local temperature and worsening the array operating margins. In such a case, dissipating the electrical power, while keeping the chip temperature suitably low, is a challenge that adds to the typical problems in cryogen-free experiments.

Due to the low bias currents, the power dissipated into conventional SIS arrays is negligible, and cryocooler integration was already demonstrated years ago [5]. This is not the case of nonhysteretic Josephson standards generating voltages varying with time, whose bias currents are in the milliampere range. Due to the high output voltage obtainable and the number of bias lines, thermal issues in such arrays are the most challenging. Nevertheless, the cryocooler cooling power, which can exceed 1 W at 4.2 K in nowadays commercial closed-cycle refrigerators, is no longer the constraining factor. The main issue is rather the capability of the thermal links from the chip (typically fabricated on a silicon substrate) to the cryocooler cold surface to dissipate the electrical power, with a limited increase in chip temperature.

At low temperature, the heat transfer between metals and dielectrics as Cu/Si strongly depends on the quality of the interfaces. For perfectly flat surfaces, the thermal boundary resistance represents the unique limitation to the heat flux [6], whereas, in the case of significantly rough surfaces, the actual contact area is reduced and the heat transfer is further limited by a bottleneck effect. It is known that the soldering of solid–solid joints represents the best solution to maximize the heat transfer at cryogenic temperature [7] since the melted solder fills very well the empty spaces between the solid surfaces. However, there are some drawbacks to this approach, as the possible degradation of the chip during the soldering, voids in

Manuscript received October 12, 2018; revised February 1, 2019; accepted February 11, 2019. Date of publication February 25, 2019; date of current version July 18, 2019. Recommended for publication by Associate Editor M. Hodes upon evaluation of reviewers' comments. *(Corresponding author: Paolo Durandetto.)*

The authors are with the Istituto Nazionale di Ricerca Metrologica, 10135 Turin, Italy (e-mail: p.durandetto@inrim.it).

Color versions of one or more of the figures in this paper are available online at http://ieeexplore.ieee.org.

Digital Object Identifier 10.1109/TCPMT.2019.2901297

2156-3950 © 2019 EU

the solder with reduced heat transfer [8], and failure due to repeated temperature cycling of the solder [9]. As an alternative, the improvement of thermal contact conductance can be achieved both by applying a suitable mechanical pressure between chip and carrier and by interposing at their interface a soft material as indium, silver, tin, or lead, which exhibits high thermal conductivity and low microhardness [10]. Mechanical pressure is a parameter that strongly affects the heat transfer between solid surfaces [11], [12] and should be controlled to obtain a good experimental reproducibility. Indium is usually preferred as thermal interface material in cryogenic applications [13], [14] as it remains soft and ductile at low temperature compensating differential thermal expansion between layers during thermal cycling.

In this paper, we present and analyze a new cryopackage design for enhancing the thermal dissipation of a PJVS chip operated in the vacuum environment of a cryocooler. Its thermal resistance has been evaluated in different operating conditions by using some PJVS segments as a known heat source, while other segments were used as a temperature sensor by measuring their critical current. The study of heat transfer dependence on the applied mechanical pressure and on temperature was carried out and is described here.

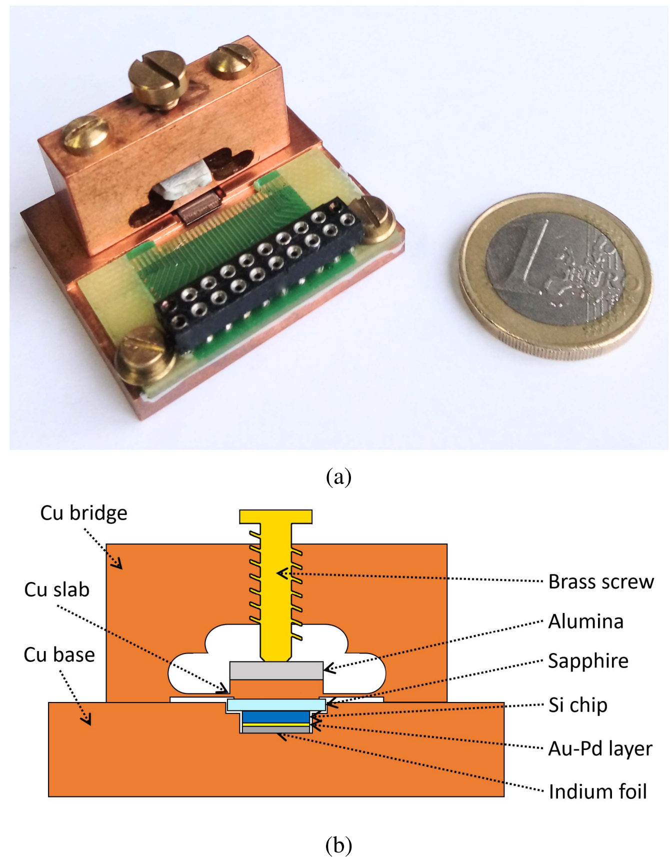

Fig. 1. (a) Special cryopackage for improved thermal dissipation and (b) its vertical front-view section (not in scale). Screw diameter and thread pitch are 4 and 0.7 mm, respectively.

II. System Setup

A. Cryopackage

The Josephson chip is enclosed in the specially designed cryopackage shown in Fig. 1(a). Its schematic cross section is also shown in Fig. 1(b), where the overall sandwich shape is clearly illustrated. The chip is fabricated on a 0.5-mm-thick Si substrate fitted inside a groove into an oxygen-free high-thermal-conductivity copper block and suitably pressed against it by a bridgelike structure designed *ad hoc*, whose section is similar to an arch closed at the bottom. A brass screw at the center of the bridge allows to press the chip against the sample holder by means of a thin Cu bottom slab, made flexible by appropriate slots. At the same time, the slab provides good thermal link to the holder. A 0.1-mm-thick Heat-Spring indium foil[1] [15] was placed between the Cu base and the chip. Furthermore, to provide a clean interface, indium oxide was mechanically removed from the In foil surface. For the same reason, the chip backside was sputter cleaned and covered by an AuPd layer of 400 nm. The upper side of the chip is electrically insulated from the Cu slab of the pressing bridge by a 0.3-mm-thick c-plane sapphire lamina, which provides an additional via for heat transmission because of its low thermal resistivity. A thin Apiezon N-layer was applied to both chip/sapphire and bridge/sapphire interfaces to further increase the heat transfer.

All these layers are then pressed against the base holder by means of the aforementioned bridge screw system. Its operation is straightforward: A calibrated torque screwdriver is used to turn the central screw and, hence, to produce a pressing force. The relationship between torque and force has been previously measured by means of a home-built calibrated load cell positioned just under the flexible slab, in place of the Cu base chip structure. In this way, the torque-to-force calibration curve of the pressing bridge was obtained, which was then used in the measurements with the Josephson chip. As shown in Fig. 1, the screw acts on an alumina spacer that, in turn, transfers the applied force to the flexible slab. The alumina spacer is used to avoid the wear of the slab as a result of the strong contact with the brass screw.

The torque-to-force relation is almost linear in the interval of our interest, whose upper force of 500 N results from an applied torque of 0.2 Nm and limits the deformation of the pressing bridge in the normal direction ($< 10\,\mu$m).

B. Josephson Chip

The PJVS chip used in this experiment was fabricated in cooperation with Physikalisch-Technische Bundesanstalt with the superconductor-normal-insulator-superconductor (SNIS) technology [16] developed for applications in quantum voltage metrology and with the peculiar characteristic in terms of the reduced temperature dependence of the electrical parameters [17]. Its operation was intensively investigated both in liquid helium and in cryocooler [18], [19]. It is made by 8192 series-connected Nb/Al-AlOx/Nb junctions, which are subdivided into 14 individually biased binary segments. This feature of PJVS arrays has been exploited in this paper

[1] Brand names are used for identification purposes. Such use implies neither endorsement by INRiM nor assurance that the equipment is the best available.

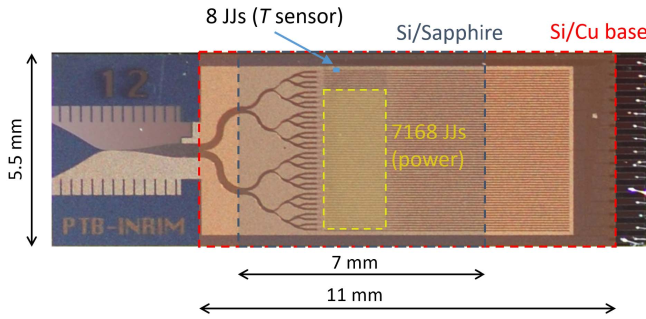

Fig. 2. 1-V SNIS PJVS array with 8192 junctions. Up to 7168 junctions (three segments, yellow dashed line) were used to generate electrical power. A single segment made up of eight junctions was used as a temperature sensing element. Red dashed line: area of the chip backside in contact with the Cu base (with In and AuPd as interfaces). Blue dashed line: area of the chip upper side in contact with the sapphire lamina (Apiezon N as an interface).

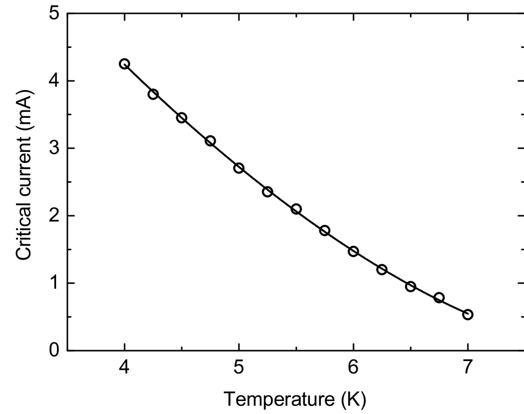

Fig. 3. Critical current versus temperature of the eight junction subarrays employed as a temperature sensor. The experimental points are fitted with a power function. More details are given in the text.

by using some segments as a power source and others as a temperature sensor, using the procedure explained in Section III and previously adopted in [20] and [21].

C. Cryogenic Apparatus and Measurement Instruments

The employed cooling system is based on a two-stage Gifford-McMahon cryocooler[2] with a minimum temperature near 2.9 K (no thermal load) and nominal cooling power of 1 W at 4.2 K. The cryocooler cold finger is fitted with an additional copper disk, the coldplate, upon which the cryopackage base is properly tightened. A thin layer of Apiezon N is applied at this Cu/Cu interface. The coldplate hosts a silicon diode thermometer and a heater wire wound around it, allowing temperature monitoring and control. A second Si thermometer, placed directly on the Cu bridge and close to the chip, is used to detect possible thermal gradients related to PJVS power dissipation.

Critical currents were evaluated from observed current to voltage dependence of array sections, obtained with a high-accuracy current source and a digital voltmeter. Additional current source and voltmeter were devoted to generate and accurately measure the electrical power dissipated in the heating junctions.

III. Measurement of Temperature Variations

To investigate the thermal behavior of our cryopackage, i.e., to evaluate its thermal resistance $R = \Delta T/P$, some of the subarrays within the PJVS (Fig. 2), counting 7168 junctions, were chosen as elements to generate a known amount of electrical power P by biasing them at currents higher than the critical current value. A single segment with eight junctions was instead used to sense the power-induced temperature variation ΔT, based on the dependence of critical current on junctions temperature. In both cases, we used a four-wire configuration that allowed to accurately estimate the generated electrical power and measure the critical current I_c of the temperature sensing junctions. To determine the chip temperature from I_c measurements, the $I_c(T)$ dependence of the sensing subarray was measured first over the relevant range in cryocooler and without extra power from the heating segments. A dc current was fed through the heater wire to vary the coldplate temperature that was measured with a calibrated sensor after it reached a stable point, i.e., after a few cryocooler time constants [22]. Chip temperature was estimated to be the same as the coldplate since very low heat is generated during I_c measurements and the gradient across its thermal resistance path to the coldplate is then negligible. The $I_c(T)$ experimental data points are shown in Fig. 3: They are well fitted by the power equation $I_c(T) = I_0\,(1 - T/T_c)^a$, with $I_0 = 12.6\,\text{mA}$, $T_c = 8.18\,\text{K}$, and $a = 1.62$. This equation has then been used for chip temperature determinations. I_c was checked before and verified at the end of all measurements.

[2]Leybold 4.2 GM.

IV. Results

A. Dependence on the Mechanical Pressure

As previously described in Section II-A, we employed the bridge screw system to exert reproducible normal forces for pressing the chip against the Cu carrier and determine the relationship with the package thermal resistance. The experimental trend of the overall thermal resistance versus the applied pressure on the Si/In/Cu contact surface ($5.5\,\text{mm} \times 11\,\text{mm} = 60.5\,\text{mm}^2$, see Fig. 2) at different temperatures is shown in Fig. 4. As expected, both mechanical pressure and operating temperature affect the thermal resistance of the cryopackage that decreases with the pressure following roughly a linear behavior.

Howe *et al.* [11] used a pressed indium foil as thermal interface material between a 10-V PJVS chip and the Cu carrier, measured $R \simeq 1.6\,\text{K}\,\text{W}^{-1}$ at 3.2 MPa and 4 K, with a contact area of $A \simeq 2\,\text{cm}^2$. To normalize R with respect to the Si/In/Cu contact surface, we evaluate the $R \cdot A$ product, a parameter independent on A. In our case, $R \cdot A = 1.9\,\text{K}\,\text{W}^{-1} \cdot 0.605\,\text{cm}^2 = 1.1\,\text{K}\,\text{cm}^2\,\text{W}^{-1}$ at 4 K and 3.2 MPa, whereas the package presented in [11] gives $R \cdot A = 3.2\,\text{K}\,\text{cm}^2\,\text{W}^{-1}$. The lower $R \cdot A$ value obtained with our cryopackage is likely due to the additional upward conduction through the sapphire layer and to the particular indium foil employed.

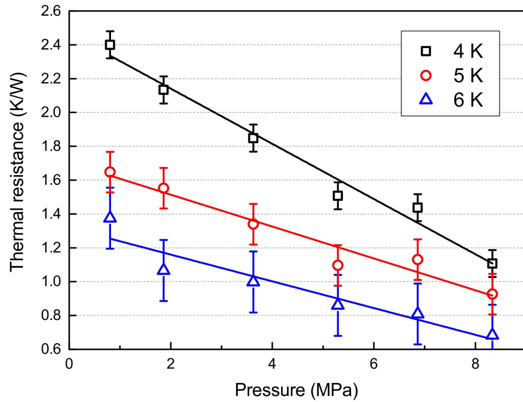

Fig. 4. Cryopackage thermal resistance versus applied mechanical pressure at different temperatures of the coldplate.

Due to the multilayered structure, the overall thermal resistance is the sum of resistances of bulk layers and interfaces between them. The thermal resistance of the thick layers in the structure can be evaluated by the simple heat transfer equation $R = (k\,S/d)^{-1}$, where k is the thermal conductivity, d is the layer thickness, and S is the layer surface. Assuming $S = 5.5\,\text{mm} \times 7\,\text{mm} = 38.5\,\text{mm}^2$ for every layer, given by the smaller contact surface in the sandwich, a worst case is studied. At 4 K, we have estimated $R \simeq 0.13\,\text{K W}^{-1}$ for the chip ($k \simeq 1\,\text{W K cm}^{-1}$ for our Si substrate [23] and $d = 0.5\,\text{mm}$) and $R \simeq 0.078\,\text{K W}^{-1}$ for sapphire ($k \simeq 1\,\text{W K cm}^{-1}$ [24] and $d = 0.3\,\text{mm}$). For Heat-Spring indium, the thermal conductivity has been obtained using the Wiedemann–Franz law, where electrical resistivity has been measured at 4 K. With $k \simeq 6\,\text{W K cm}^{-1}$ and $d = 0.1\,\text{mm}$, the thermal resistance for In is $R \simeq 0.004\,\text{K W}^{-1}$. A significant contribution could derive from the thin layers of Apiezon N at the Si/sapphire and Cu/sapphire interfaces. The thickness of the layers was estimated applying an increasing pressure between 0.5 and 6 MPa on Apiezon N flattened between the two sapphire laminae. For pressures higher than 1 MPa, the thickness was less than $1\,\mu$m, from which, with a thermal conductivity of $k \simeq 0.004\,\text{W K cm}^{-1}$ [25], a thermal resistance of about $R \simeq 0.065\,\text{K W}^{-1}$ is found. The thermal resistance of the AuPd layer is assumed to be negligible. The sum of these single-layer values of R is about $0.34\,\text{K W}^{-1}$ and is quite low compared to the experimental results shown in Fig. 4, clearly indicating that, as expected, the main contribution to the cryopackage thermal resistance derives from the interfaces.

B. Effect of the Additional Top Conduction

In this section, we want to assess the effectiveness of the sapphire lamina placed on the top of the chip as an additional heat-flow path. To this aim, we replaced it with a fused silica glass substrate of the same thickness (0.3 mm). Fused-silica thermal conductivity is around four orders of magnitude lower than sapphire one [24]; thus, it acts as a high resistance for the upward heat current.

This test has been performed with an exerted mechanical pressure of about 8.3 MPa, which corresponds to the upper

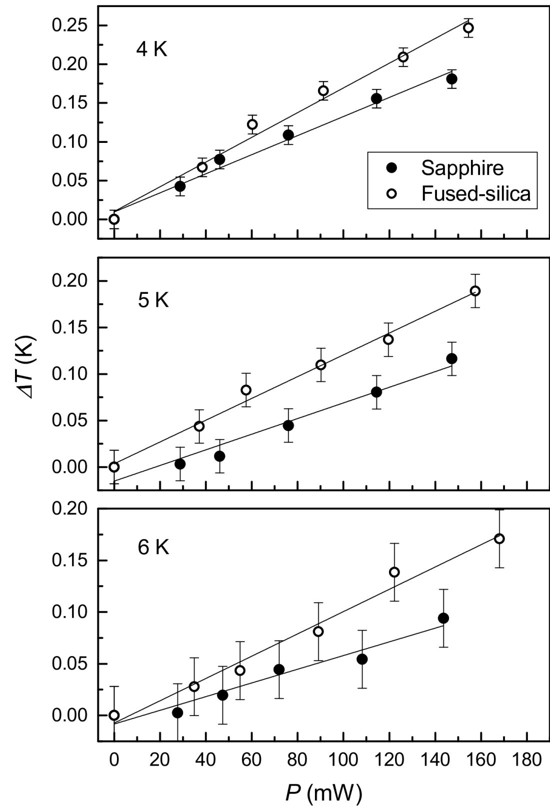

Fig. 5. Temperature increases ΔT caused by the dissipated power P with sapphire (closed circle, enabled top conduction) and fused silica glass (open circle, disabled top conduction) placed over the chip. Data were taken at different temperatures of the coldplate and with a mechanical pressure of 8.3 MPa.

TABLE I
CRYOPACKAGE THERMAL RESISTANCE CONTRIBUTIONS AT 8.3 MPa AT DIFFERENT TEMPERATURES OF THE COLDPLATE

T (K)	R_{tb} (K W^{-1})	R_b (K W^{-1})	R_t (K W^{-1})	$\frac{R_b}{R_{tb}}$
4	1.23	1.59	5.43	1.29
5	0.84	1.17	2.98	1.39
6	0.66	1.08	1.70	1.64

limit of the forces employed in the previous experiment (Section IV-A). It is important to note that the indium foil, once pressed above its yield stress (∼ 2.1 MPa), does not recover its original shape, and its reliability is guaranteed only when the applied pressure is further increased. Therefore, in order to avoid systematic errors due to the nonoptimal contact between the chip and indium, the latter was replaced with a new one in this second experiment. In Fig. 5, the temperature increase is plotted as a function of the applied electrical power in the two cases of enabled (sapphire) and disabled (fused-silica) top conduction and at different coldplate temperatures.

The cryopackage thermal system can be modeled by its analog electrical circuit, where two resistances R_t and R_b, representing, respectively, the top and the bottom paths, are connected in parallel. The equivalent resistance of such circuit R_tb is the one measured in Section IV-A with the sapphire lamina on the upper face of the chip. Replacing sapphire

TABLE II
THICKNESS VARIATION OF EACH CRYOPACKAGE ELEMENT THAT MAY CONTRIBUTE TO A PRESSURE CHANGE BETWEEN 300 AND 4 K. SEE DESCRIPTION IN THE TEXT

Element	Thickness at 300 K (mm) $d_{300\mathrm{K}}$	Thermal contraction coefficient (%) $\frac{d_{300\mathrm{K}}-d_{4\mathrm{K}}}{d_{300\mathrm{K}}}$	Variation at 4 K (µm) $\Delta = d_{300\mathrm{K}} - d_{4\mathrm{K}}$
Cu (base + bridge)	0.9 + 3 = 3.9	0.326	12.71
Brass screw	2	0.384	7.68
Alumina	1	0.064	0.64
Sapphire (or fused silica glass)	0.3	0.061 (-0.008)	0.183 (-0.024)
Si chip	0.5	0.022	0.11
In foil	0.1	0.64	0.64

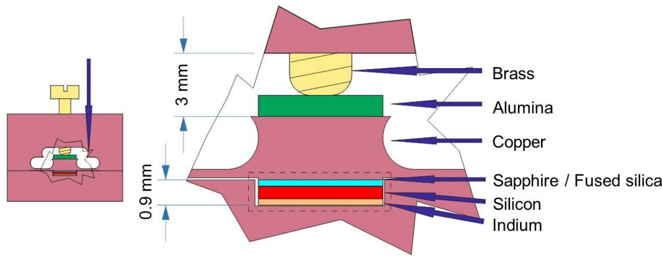

Fig. 6. Particular of the cryopackage elements that may contribute to a pressure change between 300 and 4 K.

with glass allows to determine the single bottom resistance R_{b} since the top conduction is prevented by the high thermal resistivity of fused silica. Hence, the thermal resistance of the additional heat conducting path can be evaluated by $R_{\mathrm{t}} = R_{\mathrm{tb}} R_{\mathrm{b}}/(R_{\mathrm{b}} - R_{\mathrm{tb}})$. The results are summarized in Table I and confirm that a substantial contribution to the overall heat transfer is provided by the enabled top conduction, which increases the heat transmission by lowering the cryopackage thermal resistance by 30% at 4 K up to 60% at 6 K. Since thermal resistances are dominated by interfaces, this means that, at higher temperatures, chip/sapphire and sapphire/Cu interfaces become more performing than those in the bottom path.

C. Estimation of the Actual Pressure at Low Temperature

As previously described, the chip is installed and pressed in the sample holder at room temperature and subsequently cooled down to 4 K. Therefore, the thermal contraction or expansion of the cryopackage components may cause the actual pressure to change with respect to the one applied before the cooling. A rough estimation of this effect can be obtained by using the thermal contraction coefficients to calculate the variations in height of each element of the cryopackage. Observing the scheme shown in Fig. 6, it is easy to understand that the whole Cu body may contribute to a pressure change only for 3.9 mm of its height that is the part shared with the inner elements of the package. Hence, the difference δ between the thickness change of this relevant Cu part and that of the inner components was evaluated ($\delta = \Delta_{\mathrm{Cu}} - \sum_{\mathrm{in}} \Delta_{\mathrm{in}}$). Due to its very low thickness, the contribution of the AuPd layer is neglected in this evaluation.

Table II shows the variations Δ between 300 and 4 K for each element according to the thermal expansion coefficients found in [26]–[29]. The calculated variation differences are $\delta \simeq 3.5\mu$m and $\delta \simeq 3.7\mu$m, respectively, with the sapphire and the fused silica laminae placed over the Si chip. In both cases, δ is positive, meaning that the relevant Cu part shrinks more than the internal components, which, in turn, leads to an increased pressure when the package is cooled.

The increase of mechanical pressure has been evaluated both experimentally and through simulation, assuming that is related to the deformation δ of the top of the pressing bridge in the normal direction. Using a dial gauge, we measured the relation between the vertical deformation and an exerted normal force at room temperature: An approximately linear trend has been obtained, from which follows that forces around 175 and 185 N are, respectively, required to flex the bridge by 3.5 and 3.7 μm, corresponding to mechanical pressures of 2.9 and 3.1 MPa. In order to validate these experimental findings, a SolidWorks static analysis of the cryopackage elastic deformation has been performed. In this model, the actual conditions are simplified as possible: The entire cryopackage is considered as a unique copper body and disjointed from the cryocooler coldplate. The effect of thermal contraction is simulated with an upward normal force exerting on the bridge, which then causes its deformation. As shown in Fig. 7, it has been found that a force of 200 N is required to flex the top of the bridge of about 3μm, consistent with the experimental analysis.

Both tests entail that all the measurements presented in Sections IV-A and IV-B should be corrected by adding an offset of about 3 MPa to evaluate pressure values around 4 K from that measured at room temperature. Thus, x-axis range shown in Fig. 4 should be approximately 4/11 MPa. From such a corrected graph, it is possible to derive the thermal resistance dependence on the actual pressure at low temperature, independent of the mechanical properties of the cryopackage. Regarding the comparison in Section IV-B, since the δ value in the disabled top conduction scenario (3.7μm) is slightly larger with respect to the enabled one (3.5μm), the actual pressure at low temperature turns to be higher as well. However, this difference can be neglected and, if not, it would underestimate the thermal resistances R_{b} and the performance improvement factors $R_{\mathrm{b}}/R_{\mathrm{tb}}$ listed in Table I, thus confirming our worst-case analysis.

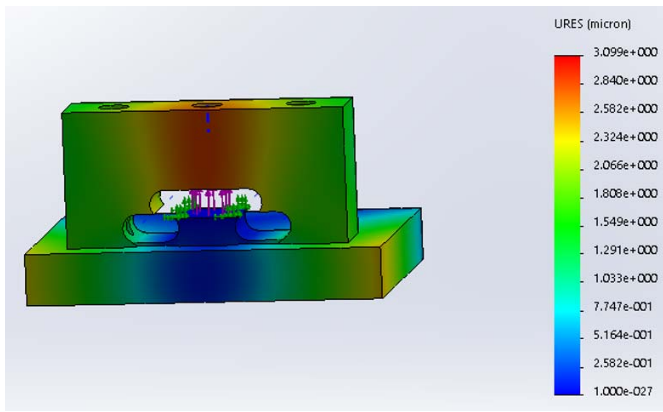

Fig. 7. Simulated cryopackage deformation due to an upward force of 200 N (purple arrows). More details are given in the text.

V. Conclusion

A special cryopackage suitable for the cryogen-free operation of programmable Josephson standards around liquid helium temperature has been designed and tested. It exploits low-temperature properties of materials, such as indium and sapphire, with a sandwich structure that noticeably enhances the dissipation of the electric power generated inside the device. A special pressing bridgelike system made of copper was designed and calibrated at room temperature to apply a known normal force to the sandwich as a way to control the thermal contact resistances of the interfaces, which are shown to be the limiting factor, assuring that the operating conditions of thermal measurement are reproducible. The actual mechanical pressure exerted at cryogenic temperature has been approximately estimated from the cryopackage thermal contraction, resulting in a nonnegligible increase with respect to the one applied at room temperature.

Although our investigation was based on a 1-V PJVS, this cryopackage can be even more effective for the 10-V PJVS that has a larger contact surface with powers up to 350 mW to be transferred to the coldplate.

Acknowledgment

The authors would like to thank B. Trinchera for providing the data acquisition system.

References

[1] B. D. Josephson, “Possible new effects in superconductive tunnelling,” *Phys. Lett.*, vol. 1, no. 7, pp. 251–253, 1962.
[2] B. M. Wood and S. Solve, “A review of Josephson comparison results,” *Metrologia*, vol. 46, no. 6, pp. R13–R20, 2009.
[3] C. J. Burroughs *et al.*, “NIST 10 V programmable Josephson voltage standard system,” *IEEE Trans. Instrum. Meas.*, vol. 60, no. 7, pp. 2482–2488, Jul. 2011.
[4] T. Melbourne, D. Cunnane, E. Galan, X. X. Xi, and K. Chen, “Study of MgB_2 Josephson junction arrays and sub-μm junctions,” *IEEE Trans. Appl. Supercond.*, vol. 25, no. 3, pp. 1–4, Jun. 2015.
[5] Y.-H. Tang *et al.*, “Cryocooled primary voltage standard system,” *IEEE Trans. Instrum. Meas.*, vol. 46, no. 2, pp. 256–259, Apr. 1997.
[6] E. T. Swartz and R. O. Pohl, “Thermal boundary resistance,” *Rev. Mod. Phys.*, vol. 61, pp. 605–668, Jul. 1989. [Online]. Available: https://journals.aps.org/rmp/abstract/10.1103/RevModPhys.61.605
[7] J. Ekin, *Experimental Techniques for Low-Temperature Measurements: Cryostat Design, Material Properties and Superconductor Critical-Current Testing*. London, U.K.: Oxford Univ. Press, 2006.
[8] H. Takahashi, M. Maruyama, Y. Amagai, H. Yamamori, N.-H. Kaneko, and S. Kiryu, “Heat transfer analysis of a programmable Josephson voltage standard chip operated with a mechanical cooler,” *Phys. C, Supercond. Appl.*, vol. 518, pp. 89–95, Nov. 2015.
[9] R. K. Kirschman, W. M. Sokolowski, and E. A. Kolawa, “Die attachment for −120 °C to +20 °C thermal cycling of microelectronics for future mars rovers—An overview,” *J. Electron. Packag.*, vol. 123, no. 2, pp. 105–111, 2001.
[10] I. Savija, J. R. Culham, M. M. Yovanovich, and E. E. Marotta, “Review of thermal conductance models for joints incorporating enhancement materials,” *J. Thermophys. Heat Transf.*, vol. 17, no. 1, pp. 43–52, 2003.
[11] L. Howe, C. J. Burroughs, P. D. Dresselhaus, S. P. Benz, and R. E. Schwall, “Cryogen-free operation of 10 V programmable Josephson voltage standards,” *IEEE Trans. Appl. Supercond.*, vol. 23, no. 3, Jun. 2013, Art. no. 1300605.
[12] L. J. Salerno, P. Kittel, and A. L. Spivak, “Thermal conductance of pressed metallic contacts augmented with indium foil or apiezon grease at liquid helium temperatures,” *Cryogenics*, vol. 34, no. 8, pp. 649–654, 1994.
[13] M. Deutsch, “Thermal conductance in screw-fastened joints at helium temperatures,” *Cryogenics*, vol. 19, no. 5, pp. 273–274, 1979. [Online]. Available: https://www.sciencedirect.com/science/article/abs/pii/0011227579901413
[14] A. Dillon, K. McCusker, J. V. Dyke, B. Isler, and M. Christiansen, “Thermal interface material characterization for cryogenic electronic packaging solutions,” in *Proc. IOP Conf. Ser., Mater. Sci. Eng.*, 2017, vol. 278, no. 1, Art. no. 012054.
[15] *Indium Corporation*. [Online]. Available: https://www.indium.com/thermal-interface-materials/heat-spring/#products
[16] V. Lacquaniti, N. De Leo, M. Fretto, A. Sosso, F. Müller, and J. Kohlmann, “1 V programmable voltage standards based on SNIS Josephson junction series arrays,” *Supercond. Sci. Technol.*, vol. 24, no. 4, p. 045004, 2011.
[17] A. Sosso, B. Trinchera, E. Monticone, M. Fretto, P. Durandetto, and V. Lacquaniti, “Temperature stability of SNIS Josephson arrays between 4.2 K and critical temperature in cryocooler,” *IEEE Trans. Appl. Supercond.*, vol. 25, no. 3, pp. 1–4, Jun. 2015.
[18] A. Sosso, P. Durandetto, B. Trinchera, M. Fretto, E. Monticone, and V. Lacquaniti, “Cryogen-free operation of SNIS for AC quantum voltage standards,” *IEEE Trans. Appl. Supercond.*, vol. 26, no. 3, pp. 1–3, Apr. 2016.
[19] B. Trinchera, V. Lacquaniti, A. Sosso, M. Fretto, P. Durandetto, and E. Monticone, “On the synthesis of stepwise quantum waves using a SNIS programmable Josephson array in a cryocooler,” *IEEE Trans. Appl. Supercond.*, vol. 27, no. 4, pp. 1–5, Jun. 2017.
[20] R. E. Schwall, D. P. Zilz, J. Power, C. J. Burroughs, P. D. Dresselhaus, and S. P. Benz, “Practical operation of cryogen-free programmable Josephson voltage standards,” *IEEE Trans. Appl. Supercond.*, vol. 21, no. 3, pp. 891–895, Jun. 2011.
[21] M. Schubert *et al.*, “A dry-cooled AC quantum voltmeter,” *Supercond. Sci. Technol.*, vol. 29, no. 10, p. 105014, 2016.
[22] A. Sosso and P. Durandetto, “Experimental analysis of the thermal behavior of a GM cryocooler based on linear system theory,” *Int. J. Refrig.*, vol. 92, pp. 125–132, Aug. 2018. [Online]. Available: https://www.sciencedirect.com/science/article/pii/S0140700718301221
[23] M. Asheghi, K. Kurabayashi, R. Kasnavi, and K. E. Goodson, “Thermal conduction in doped single-crystal silicon films,” *J. Appl. Phys.*, vol. 91, no. 8, pp. 5079–5088, 2002.
[24] S. W. Van Sciver, *Helium Cryogenics*. New York, NY, USA: Springer, 2012.
[25] M. M. Kreitman and J. T. Callahan, “Thermal conductivity of apiezon N grease at liquid helium temperatures,” *Cryogenics*, vol. 10, no. 2, pp. 155–159, 1970.
[26] G. Ventura and L. Risegari, *The Art of Cryogenics: Low-Temperature Experimental Techniques*. New York, NY, USA: Elsevier, 2010.
[27] R. J. Corruccini and J. J. Gniewek, *Thermal Expansion of Technical Solids at Low Temperatures: A Compilation From the Literature*. Washington, DC, USA: United States Government Printing Office, 1961
[28] C. A. Swenson, “Properties of indium and thallium at low temperatures,” *Phys. Rev. J. Arch.*, vol. 100, no. 6, p. 1607, 1955.

[29] N. J. Simon, "Cryogenic properties of inorganic insulation materials for ITER magnets: A review," Nat. Inst. Standards Techn., Boulder, Colorado, USA, Tech. Rep. NISTIR-5030, 1994.

Paolo Durandetto was born in 1986. He received the M.Sc. degree in physics of fundamental interactions from the University of Turin, Turin, Italy, in 2011. His M.Sc. thesis was on the application of cosmic rays for the detection of high atomic number materials. He is currently pursuing the Ph.D. degree in metrology with the Istituto Nazionale di Ricerca Metrologica, Turin, in collaboration with the Polytechnic University of Turin.

In 2014, he joined the Istituto Nazionale di Ricerca Metrologica. His current research interests include the application of Josephson devices for the synthesis of ac and arbitrary voltage in closed-cycle refrigeration systems.

Eugenio Monticone was involved in superconductors film deposition of Nb and MgB2 for the realization of Josephson junctions, bolometers for the visible, infrared, and microwaves, and sensors for the ac–dc transfer, study and fabrication of transition-edge sensors for single-photon counters and optimization of He-free system for the metrology application of Josephson array. He is currently a Senior Researcher with the Istituto Nazionale di Ricerca Metrologica, Turin, Italy, where he is involved in the realization and characterization of superconductive devices for precision measurements. He has authored or coauthored more than 100 peer-reviewed papers.

Danilo Serazio was born in Ivrea, Turin, Italy, in 1966. He received the Technical School degree from the Istituto Don Bosco, Rivarolo, Turin, Italy, in 1982, and the High School Degree in electronics from the Istituto Tecnico Industriale "A. Avogadro," Turin, in 1999.

In 1995, he joined the Istituto Nazionale di Ricerca Metrologica, Turin, where he is currently with the Quantum Metrology and Nanotechnologies Department. He is involved in the electrical power/energy measurement activity and in the development of mechanical and electrical equipment for ac and dc measurements.

Andrea Sosso received the Ph.D. degree from the Polytechnic University of Turin, Turin, Italy, in 1993.

He has been with the Istituto Nazionale di Ricerca Metrologica, Turin, where he developed Josephson standards of dc/ac voltage and quantum Hall effect for ac resistance, measurement systems for fundamental constants determination, dedicated cryogenics, optical setups and electronics for both electrical and dimensional metrology. He has authored or coauthored more than 100 peer-reviewed publications. He holds four patents.

Dr. Sosso is a member of several Italian and international committees. He has led the participation in several international projects and acted as a referee for international journals, conferences, and research projects.